

# Photoluminescence Stokes shift and exciton fine structure in CdTe nanocrystals

J. Pérez-Conde

*Departamento de Física, Universidad Pública de Navarra, E-31006 Pamplona, Spain*

A. K. Bhattacharjee

*Laboratoire de Physique des Solides, UMR du CNRS,  
Université Paris-Sud, 91405 Orsay, France*

M. Chamarro and P. Lavallard

*Groupe de Physique des Solides, Universités Paris VI et VII,  
CNRS UMR 7588, 2 Place Jussieu, 75251 Paris, France*

V. D. Petrikov and A. A. Lipovskii

*St. Petersburg State Technical University,  
Polytechnicheskaja 29, St. Petersburg 19251, Russian Federation*

## Abstract

The photoluminescence spectra of spherical CdTe nanocrystals with zincblende structure are studied by size-selective spectroscopic techniques. We observe a resonant Stokes shift of 15 meV when the excitation laser energy is tuned to the red side of the absorption band at 2.236 eV. The experimental data are analyzed within a symmetry-based tight-binding theory of the exciton spectrum, which is first shown to account for the size dependence of the fundamental gap reported previously in the literature. The theoretical Stokes shift presented as a function of the gap shows a good agreement with the experimental data, indicating that the measured Stokes shift indeed arises from the electron-hole exchange interaction.

PACS numbers: 71.35.Cc, 73.22.-f, 78.55-m, 78.66.Hf

Three-dimensional confinement in semiconductor nanocrystals (NC's), also called quantum dots (QD's), leads to a discretization of the electronic energy levels and a blue shift of the absorption edge. The confinement also enhances the electron-hole direct and exchange Coulomb interactions because the spatial overlap of the electron and hole wave functions strongly increases with decreasing size. As a consequence, the fine structure splittings of the lowest-energy excitonic states are much larger than in the bulk material.<sup>1</sup> Evidence of such enhanced splittings in the photoluminescence (PL) Stokes shifts was reported<sup>2,3</sup> in CdSe NC's and more recently<sup>4</sup> in CdS NC's. In both semiconductors, the Stokes shift between the energy of the resonantly excited first electron-hole state and the luminescence line is about 10 meV in NC's of radius 15 Å. It arises from an interplay of the electron-hole exchange interaction and the crystal-field term in the wurtzite structure CdSe, while the small spin-orbit interaction plays an important role in CdS. In this paper we study zincblende CdTe NC's, where the exciton fine structure is expected to be completely determined by the electron-hole interaction. We first present an experimental determination of the size-dependent Stokes shift. A theoretical model based on the tight-binding (TB) method is then used to analyze the data. It is shown to account for the available data on the size-dependent absorption gap. Finally, we present a comparison between the calculated Stokes shift as a function of the gap and our measured values, showing an excellent agreement.

We report a detailed analysis of the fine structure of the photoluminescence (PL) spectra observed under resonant excitation. Optical absorption measurement was performed with a Cary 2300 spectrometer. Non-resonant photoluminescence excitation was realized with the green line of an Ar<sup>+</sup> laser at 514 nm. Resonant PL was obtained with a Coumarin 6 dye-laser pumped by the 488 nm line of an Ar<sup>+</sup> laser. The PL spectra were analyzed with double substrative spectrometer which minimizes the rate of diffused light. The spectral resolution was 1 meV.

The sample studied is a phosphate P<sub>2</sub>ONa<sub>2</sub>O-ZnO-AlF<sub>3</sub>-Ga<sub>2</sub>O<sub>3</sub> glass containing ~ 1.2 wt.% of CdTe. The synthesis of the material was achieved following a process previously described.<sup>5</sup> The technique of raw batch was applied. Closed crucible technique was used to prevent decreasing Te concentration through volatility. After the synthesis and the quenching at 300°C the glass samples were properly annealed to grow CdTe nanocrystals of necessary size.

Low-temperature absorption and non-resonant PL spectra are represented in Fig. 1. The

absorption spectrum show a very broad maximum at an energy of 2.25 eV. Three maxima are clearly observed in the non-resonant PL spectrum. The maximum of the highest energy PL band matches very well the first energy maximum of the absorption spectrum indicating the intrinsic origin of this PL band. The two lowest energy maxima of PL spectrum should be attributed to the recombination from states in the energy band gap.

By tuning the laser energy to the red side of the lowest energy absorption band, one excites only the lowest energy transitions of the biggest nanocrystals. Fig. 2 shows a spectrum obtained in this condition. The spectrum (resonant PL) reveals fine structures which were not present in the emission spectrum from the whole distribution (non-resonant PL). Three peaks are superimposed on the high-energy side of the broad band peaked at 2.125 eV (see Fig. 1). The first peak is shifted with respect to the energy laser excitation (2.236 eV) to the red by about 15 meV. The other two peaks are the 1LO and 2LO phonon replica of the first peak. When the excitation energy is changed from 2.193 to 2.306 eV the red shift of the first peak increases from 13 meV up to 20 meV (with an accuracy equal to  $\pm 1$  meV).

Previous theoretical studies of the exciton structure based on the effective mass approximation (EMA),<sup>3</sup> pseudopotential,<sup>6</sup> and tight-binding methods.<sup>7,8</sup> have been mostly devoted to CdSe NC's, where the crystal-field term also plays an important role. Here we apply a recently developed symmetry-based TB theory<sup>10</sup> to zincblende CdTe NC's. It is based on the semi-empirical  $sp^3s^*$  TB model of Vogl *et al.*<sup>9</sup> extended to include the spin-orbit interaction, which accounts for the main features of the bulk semiconductor band structure. We first deduce the complete single-particle spectrum in a QD of  $T_d$  symmetry by using group-theoretical methods.<sup>10</sup> The TB parameters for CdTe in the present paper are taken from Ref. 11:  $E_{s,a} = -9.86$ ,  $E_{p,a} = -0.04$ ,  $E_{s,c} = 0.4$ ,  $E_{p,c} = 5.26$ ,  $V_{s,s} = -3.71$ ,  $V_{x,x} = 1.22$ ,  $V_{x,y} = 4.12$ ,  $V_{s,p} = 0.54$ ,  $V_{p,s} = -4.81$ ,  $E_{s^*,a} = 7.0$ ,  $E_{s^*,c} = 8.50$ ,  $V_{s^*,p} = 2.46$ ,  $V_{p,s^*} = -0.67$ ,  $\lambda_a = 0.3285$  and  $\lambda_c = 0.0591$  eV. Where  $E_{ib}$  are the effective atomic energy levels for cations ( $b = c$ ) and anions ( $b = a$ ),  $V_{ij}$  are the hopping parameters between the  $i$  and  $j$  orbitals on nearest-neighbor atoms and  $\lambda_b$  are the spin-orbit coupling parameters. We consider quasi-spherical crystallites of zincblende structure ranging from 17.81 Å (87 atoms) to 58.68 Å (3109 atoms) in diameter. The dangling bonds are saturated by hydrogen atoms with the H energy level at  $E_{s,H} = -10$  eV. The hydrogen-to-atom bond lengths are chosen so that the surface states have completely disappeared from the gap and relevant states below and

above it. In this work the cation-hydrogen and anion-hydrogen bond lengths have been fixed at  $d_{Cd-H} = 0.81$  and  $d_{Te-H} = 0.77$  Å respectively. A more detailed discussion on the dangling bond saturation in CdTe nanocrystals was presented previously.<sup>10</sup>

The TB Hamiltonian is written in a block-diagonal form by using a symmetrized basis corresponding to the double-valued representations  $\Gamma_6$ ,  $\Gamma_7$  and  $\Gamma_8$  of the tetrahedral group  $T_d$ . An exact diagonalization then yields the one-particle QD eigenstates  $\phi_i$ , which can be finally written as

$$\phi_i(\mathbf{r}) = \sum_{R,k,m} C_{R,k,m}^i u_m^k(\mathbf{r} - \mathbf{R}), \quad (1)$$

where  $\mathbf{R}$  denotes the atomic site and  $u_m^k$  represent the spin-orbit coupled symmetrized atomic orbitals, with  $k = 6, 7, 8$  for  $\Gamma_6$ ,  $\Gamma_7$ ,  $\Gamma_8$  representations respectively. Let us summarize the essential features of our results. The two highest occupied valence levels are near each other in energy and belong to the  $\Gamma_8$  (fourfold degenerate) symmetry. Additionally, for the three biggest NC's studied here, these two levels are well separate in energy from the others (see Table I). The dominant orbital symmetry of the highest level is  $\Gamma_5$  for the NC sizes considered here and the nearest level presents also a non-zero  $\Gamma_5$  orbital contribution. This is in contrast with the EMA results where one of the two highest valence levels is dipole allowed and the other is forbidden.<sup>12</sup> The symmetry of the lowest conduction state is  $\Gamma_6$  and almost pure  $\Gamma_1$  in its orbital part. Furthermore, the next conduction level is well separated in energy. That means that the lowest energy part of optical transitions will be driven essentially by the two  $\Gamma_8$  valence quadruplets and the  $\Gamma_6$  conduction doublet (see Table I).

From the single-particle states we can now write the exciton states in terms of Slater determinants. Formally,  $|e\rangle = \sum_{v,c} C_{v,c} |v, c\rangle$ , where  $|v, c\rangle = a_c^\dagger a_v |g\rangle$  and the  $a_c^\dagger(a_v)$  is the creation(annihilation) operator for a conduction (valence) electron and  $|g\rangle$  represents the many-body ground state corresponding to the fully occupied valence bands. When the  $e - e$  Coulomb interaction is introduced the matrix elements of the total Hamiltonian can be written as,

$$H_{vc,v'c'} = (\varepsilon_c - \varepsilon_v) \delta_{vv'} \delta_{cc'} - J_{vc,v'c'} + K_{vc,v'c'}, \quad (2)$$

with  $J$  and  $K$  representing the direct and exchange terms respectively. When  $J$  and  $K$  are written in terms of the QD single-particle states in Eq. (1), each of them contain many direct and exchange integrals of atomic orbitals. After standard simplifying approximations (see Refs. 7 and 8 for details), the unscreened on-site Coulomb and exchange integrals for

anion (cation) are assumed to be  $U_{coul} = 13(10.5)$  eV and  $U_{exch} = 1(0.5)$  eV respectively. These values follow roughly those obtained for CdSe.<sup>7,8</sup> The values for the Te atom have been calculated by means of a simple scaling. Finally, the integrals are screened in the Coulomb terms  $J$ , but left unscreened up to the nearest neighbors in the exchange terms  $K$ . The on-site screening factor is taken to be 0.4 and 0.5 for cation and anion respectively. The nearest-neighbor exchange integrals are assumed one tenth of the on-site ones. The size dependent permittivity appearing in  $J$  and  $K$  follows the model given by Wang and Zunger<sup>13</sup> for CdSe NC's. In particular, the size dependent permittivity in the five NC's analyzed here with diameters 17.81, 24.95, 32.43, 43.02 and 58.68 Å is given by 6.14, 6.64, 7.09, 7.68 and 8.54 respectively.

In order to derive the fine structure of the lowest-energy interband transitions, we diagonalized the full exciton Hamiltonian in a subspace of progressively increasing size, with as many valence and conduction states as necessary to reach numerical convergence. We needed up to 18 valence and 14 conduction states respectively for achieving a convergence to 0.1 meV for the energy shifts of the eight lowest states.

The most important contributions to the lowest part of the exciton spectrum come from the 16 Slater determinants which correspond to the direct products of the highest two  $\Gamma_8$  valence states and the the lowest  $\Gamma_6$  conduction states. When the Hamiltonian diagonalization is restricted to the Hilbert space spanned by these 16 states the results are close to those reached at the numerical convergence. The essential physics of the lowest excitations can be extracted, however, from the eight lowest exciton states: The symmetry structure of these levels is not changed after convergence. We find an optically inactive doublet ground state ( $\Gamma_3$  symmetry). The first excited state is a forbidden triplet ( $\Gamma_4$ ), which is almost degenerate with the doublet. Finally, the second excited state is an optically active triplet ( $\Gamma_5$ ). It is interesting to note that the above level scheme indeed corresponds to the splitting expected from the electron-hole exchange interaction.

The absorption gap is obtained numerically from the first allowed energy level in the excitonic space, the  $\Gamma_5$  triplet. The numerical results along with the collected experimental data are shown in Fig. 3.

In our resonant PL experiment the laser excitation creates an optically active exciton state (the  $\Gamma_5$  triplet). After relaxation, the luminescence is emitted by recombination from the exciton ground state (the  $\Gamma_3$  doublet). The resonant Stokes shift,  $\Delta_{exch}$ , is obtained

from the energy difference between these two levels. The theoretical results along with the experimental data from the shift between the excitation energy and the luminescence peak are presented in Fig. 4 and show an excellent agreement. By looking the Table I, it is easy to verify that the observed Stokes shift of 15 meV cannot be interpreted in terms of the energy separation between the highest two valence levels.

When we plot the calculated Stokes shift against the NC diameter the results are rather close to those from the EMA calculations of Efros *et al.*<sup>3</sup> However, a more recent EMA theory<sup>14</sup> which includes the long-range part of the electron-hole exchange interaction, yields larger Stokes shift values.<sup>15</sup>

In conclusion, we report the observation of a sizeable resonant Stokes shift in the photoluminescence from CdTe nanocrystals. The experimental data show an excellent agreement with the exciton fine structure calculated in a TB theory which also accounts for the size dependence of the absorption gap. Moreover, the theoretical analysis indicates that the observed Stokes shift arises from the electron-hole exchange interaction.

Diameter (Å)	$v_1$	$v_2$	$v_3$	$c_1$	$c_2$
17.81.	-0.579(8)	-0.799(8)	-0.897(8)	2.747(6)	2.957(6)
24.95	-0.330(8)	-0.464(8)	-0.558(8)	2.466(6)	2.860(7)
32.43	-0.270(8)	-0.341(8)	-0.453(8)	2.097(6)	2.408(7)
43.08	-0.154(8)	-0.191(8)	-0.273(8)	1.972(6)	2.225(7)
58.67	-0.093(8)	-0.110(8)	-0.168(8)	1.823(6)	1.997(7)

Table I: Energy values of the three highest valence and the two lowest conduction levels in eV. The symmetries are indicated in parentheses.

- 
- <sup>1</sup> P. D. J. Calcott, K. J. Nash, L. T. Canham, M. J. Kane, and D. Brumhead, *J. Phys. Condens. Matter* **5**, L91 (1993).
- <sup>2</sup> M. Chamarro, C. Gourdon, P. Lavallard, O. Lublinskaya, and A. I. Ekimov, *Phys. Rev. B* **53**, 1336 (1996).
- <sup>3</sup> A.I. L. Efros, M. Rosen, M. Kuno, M. Nirmal, D. J. Norris, and M. G. Bawendi, *Phys. Rev. B* **54**, 4843 (1996).
- <sup>4</sup> M. Chamarro, M. Dib, V. Voliotis, A. Filoramo, P. Rousignol, T. Gascoin, J. P. Boilot, C. Delerue, G. Allan, and M. Lannoo, *Phys. Rev. B* **57**, 3729 (1998).
- <sup>5</sup> E. K. Kolobkova, A. A. Lipovskii, and V. D. Petrikov, *J. Crystal Growth* **184-185**, 365 (1998).
- <sup>6</sup> A. Franceschetti, H. Fu, L. W. Wang, and A. Zunger, *Phys. Rev. B* **60**, 1819 (1999).
- <sup>7</sup> J. Pérez-Conde and A. K. Bhattacharjee, to be published.
- <sup>8</sup> K. Leung, S. Pockrant, and K. B. Whaley, *Phys. Rev. B* **57**, 12 291 (1998).
- <sup>9</sup> P. Vogl, H. P. Hjalmarson, and J. D. Dow, *J. Phys. Chem. Solids* **44**, 365 (1983).
- <sup>10</sup> J. Pérez-Conde and A. K. Bhattacharjee, *Solid State Comm.* **110**, 259 (1999).
- <sup>11</sup> D. Bertho (unpublished), cited by V. Albe, Doctoral thesis, Université Montpellier II (1997).
- <sup>12</sup> T. Richard, P. Lefebvre, H. Mathieu, and J. Allègre, *Phys. Rev. B* **53**, 7287 (1996)
- <sup>13</sup> L. W. Wang and A. Zunger, *Phys. Rev. B*, **53**, 9579 (1996).
- <sup>14</sup> S. V. Goupalov and E. L. Ivchenko, *J. Crystal Growth* **184-185**, 393 (1998); S. V. Gupalov and E. L. Ivchenko *Phys. Solid State* **42**, 2030 (2000).
- <sup>15</sup> P. Lavallard and G. Lamouche (unpublished).
- <sup>16</sup> T. Rajh, O. I. Mičić, and A. J. Nozik, *J. Phys. Chem. B* **97**, 11999 (1993).
- <sup>17</sup> Y. Mastai and G. Hodes, *J. Phys. Chem. B* **101**, 2685 (1997).
- <sup>18</sup> Y. Masumoto and K. Sonobe, *Phys. Rev. B* **56**, 9734 (1997).
- <sup>19</sup> H. Arizpe-Chávez, R. Ramírez-Bon, F. J. Espinoza-Beltrán, O. Zelaya-Angel, J. L. Marín, and R. Riera, *J. Phys. Chem. of Solids* **61**, 511 (2000).
- <sup>20</sup> A. M. Kapitonov, A. P. Stupak, S. V. Gaponenko, E. P. Petrov, A. L. Rogach, and A Eychmüller, *J. Phys. Chem. B* **103**, 10109 (1999).

Figure 1: Low temperature absorption (dashed line) and non-resonant PL spectra (solid line).

Figure 3: Absorption band gap versus QD diameter. The experimental data were taken at different temperatures. The data from Ref. 16 (open diamonds) and Ref. 17 (closed squares) were measured at the room temperature. The data from Ref 18 (stars) were measured in superfluid helium at 2 K. The values from Ref. 19 were taken at temperatures higher than room temperature (open circles). Finally the sample studied in Ref. 20 (closed circles) was measured at 77 K (higher value) and room temperature (lower value). Our theoretical TB values scale (open triangles) as a function of the diameter as  $1/D^{1.42}$ , while the EMA<sup>12</sup> gap (dotted line) varies as  $1/D^2$ .

Figure 4: The resonant Stokes shift is plotted against the absorption gap. The experimental values (open circles) and the calculated ones (open triangles) are compared.

Figure 2: Photoluminescence spectrum from selective excitation at 2.223 eV.



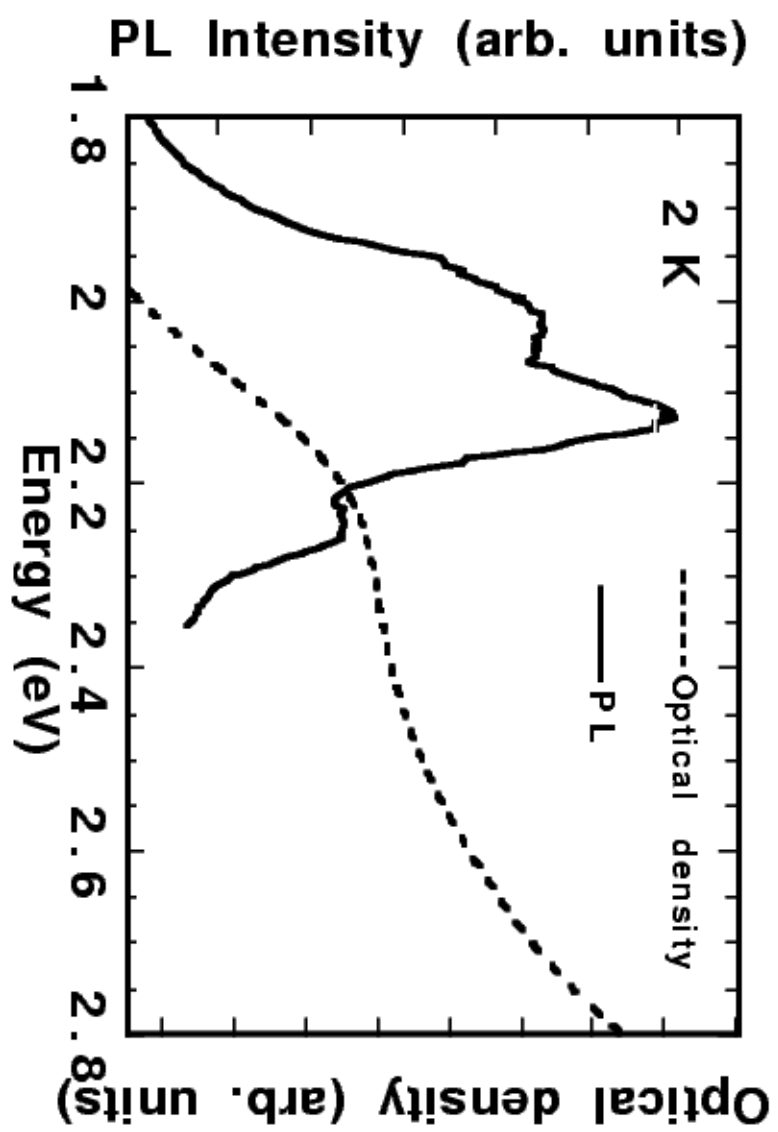


Fig. 1

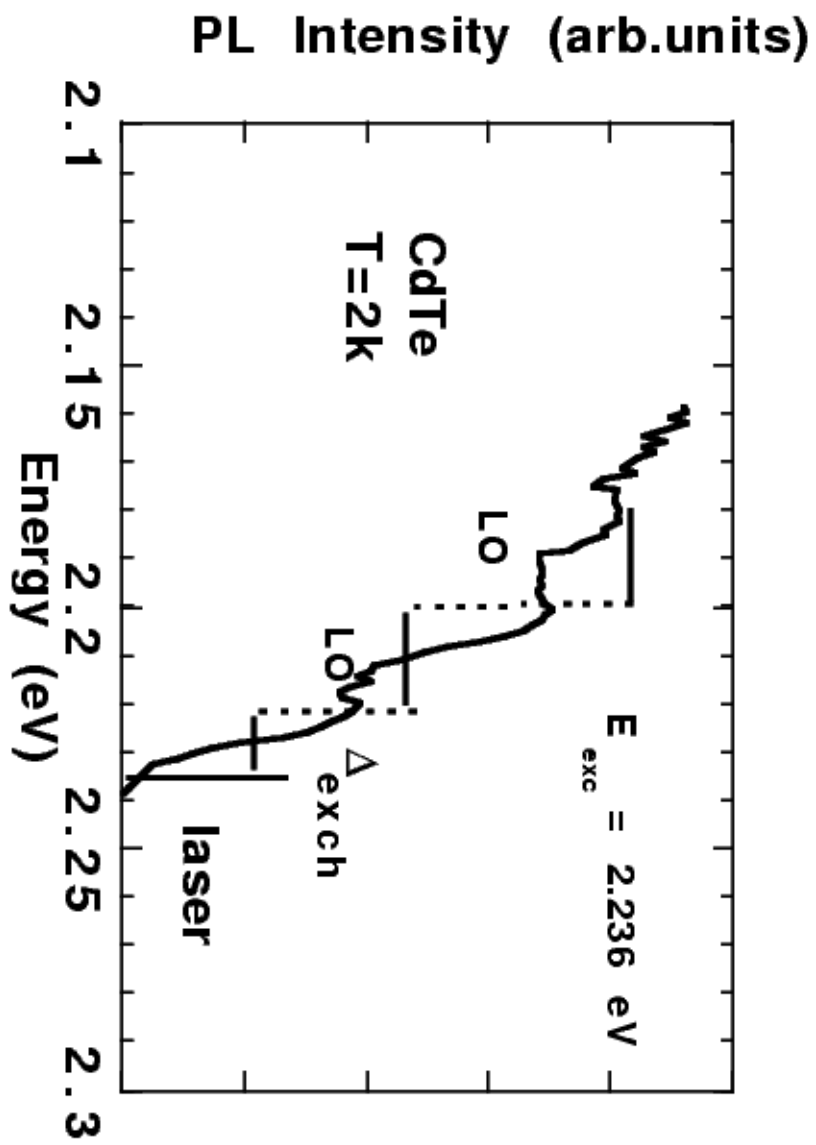


Fig. 2

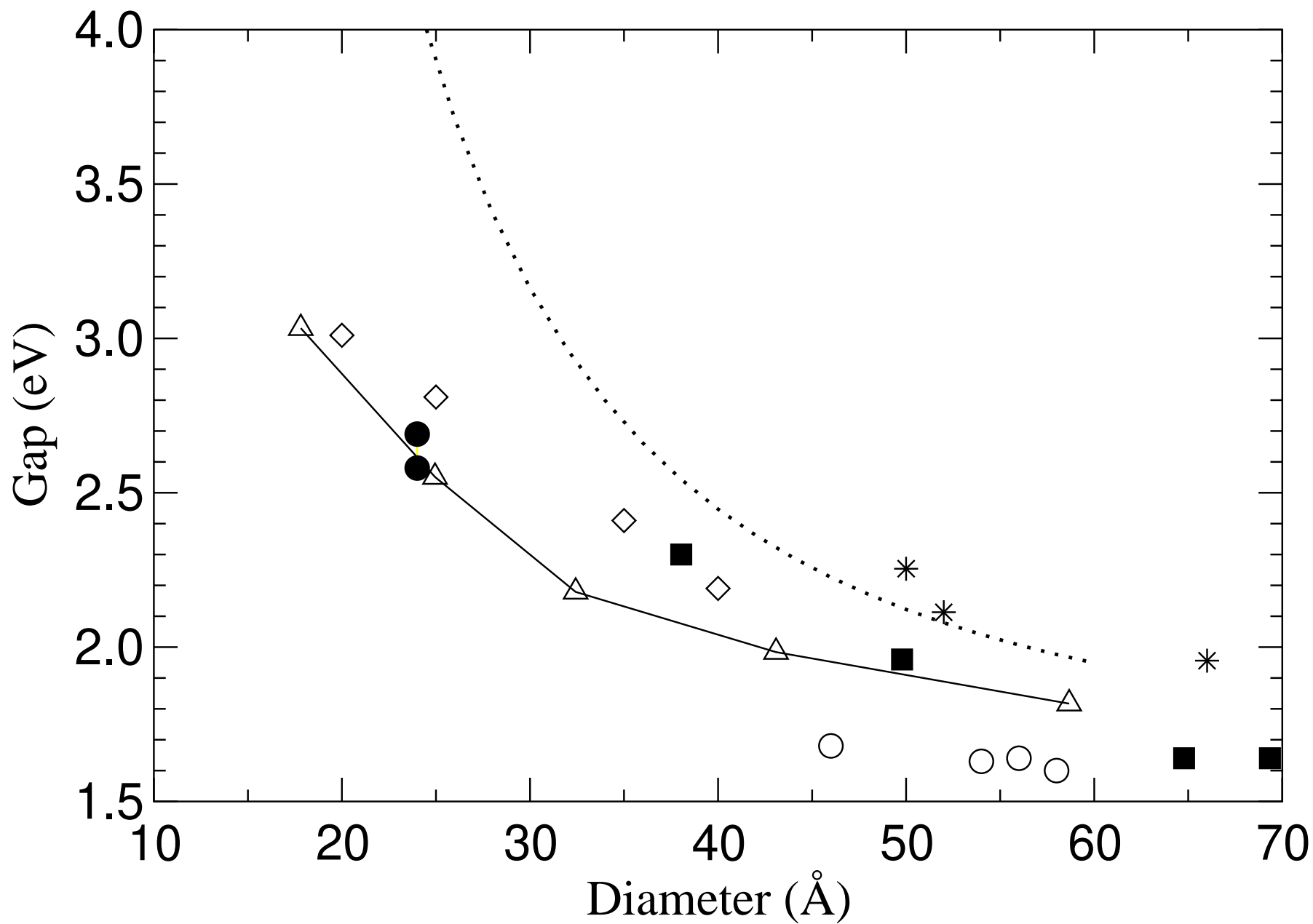


Fig. 3

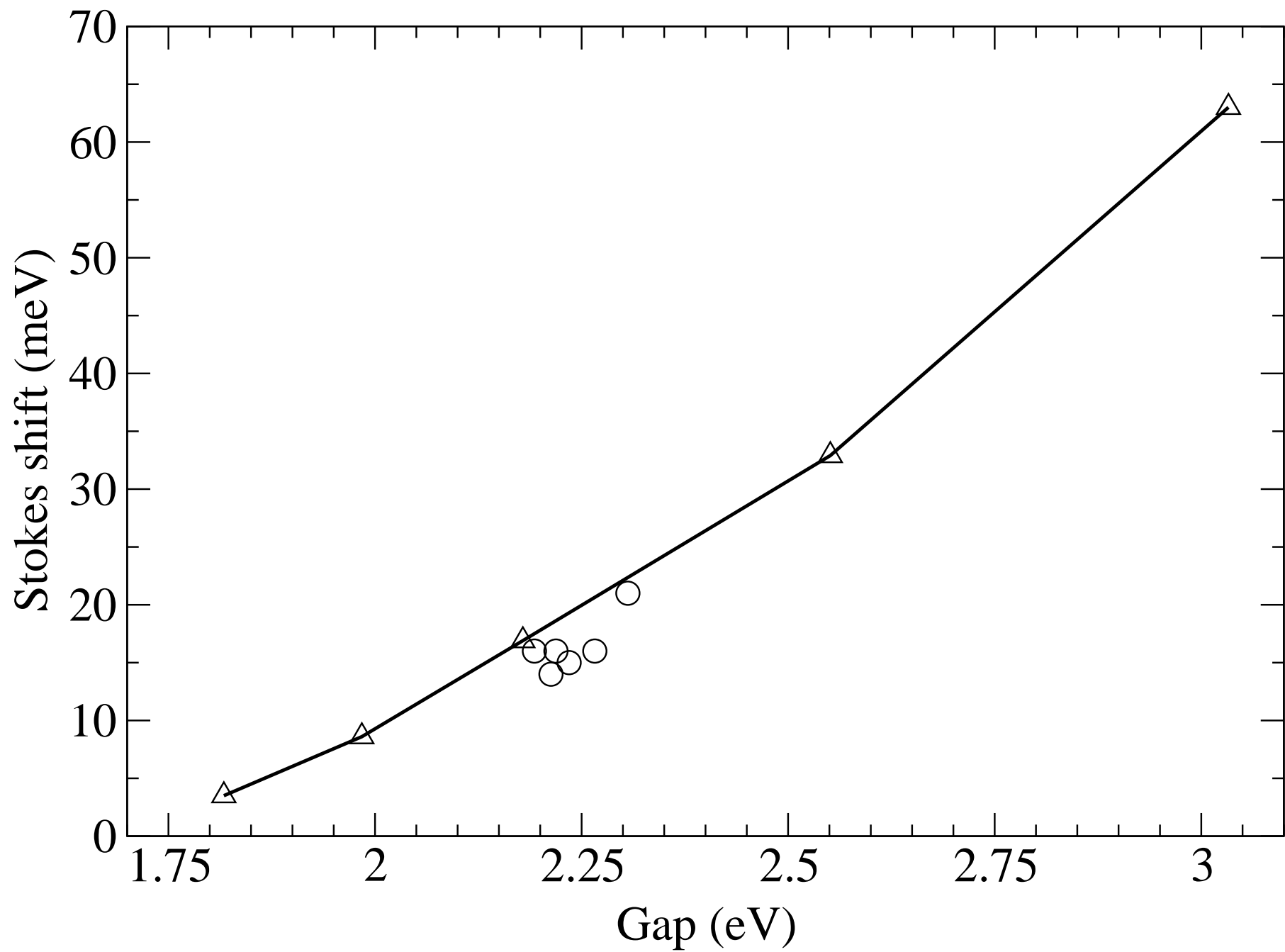


Fig. 4